PIEZO-RESISTIVE MEMS PRESSURE SENSOR
FOR TIRE BEAD SEATING PRESSURE MEASUREMENT:
DESIGN, SIMULATION, ANALYSIS AND FABRICATION PROCESS

[1]Kusuma N and [2]Sujit ES

[1] Sensor and Vision Technology Deaprtment
Central Manufacturing Technology Institute, Bengaluru
[2]Department of Instrumentation and Control Engineering
SRM University, Kattankulathur, Tamil Nadu
[1]E-mail: kusuma.cmti@nic.in

Abstract: *Understanding the tire behavior during tire inflation is critical to design a high- performance tire. To improve handling and response, tire manufacturers need to understand the changes of a tire under various conditions. A MEMS pressure sensor can be placed on the rim to make contact with the tire bead, and can measure the pressure distribution of a tire across the sensor face. Considering the unique nature of each sensor and the trade-offs in design, it is not feasible to follow a standard design approach. Thus, it is useful to derive the specific design, considering number of important factors to arrive at the 'ideal' design. The selection of appropriate parameters of piezoresistors such as the shape and the position of the piezoresistor on the pressure sensor diaphragm, thickness of diaphragm are important. This research work shows the scope of using analytical solutions and design techniques for a development of piezoresistive pressure sensor. This research work also focuses on piezoresistive pressure sensor principles, design, modeling, parameters to be considered, materials that can be used in MEMS fabrication. Here the MEMS fabrication process has been discussed in brief pertaining to the application and feature size. Few models of piezoresistive based MEMS pressure sensors have been simulated, analysed and the results are presented.*

Index Terms: *Piezoresistivity, Sensitivity, Pressure Sensor, MEMS*

1. INTRODUCTION

This paper has been presented in a lucid form for easy understanding over 5 sections. Section - I introduce to the paper and provide an insight on the topic. Section II focuses on the literature about design principles such as piezoresistivity, piezoresistive effect, proof pressure, burst pressure and dynamic response of pressure sensor. Section III briefs on mathematical modeling and design calculations of the piezoresistive pressure sensors and the design considerations and MEMS fabrication process flow are discussed. Section IV discusses briefly about the simulations and results for optimized design selected. This paper has been concluded at Section V with the inference and observations from the Simulation and Analysis of designed Piezoresistive Pressure sensor for bead seating pressure measurement of 0 to 15bar pressure.

The domain of silicon piezo-resistive pressure sensors has been through major technology make-over over the past four decades in terms of design methodology and fabrication processes. Considering the unique nature of each sensor and the trade-offs in design, it is not feasible to follow a standard design approach. Thus, it is required to derive the specific design considering number of important factors to arrive at the best design. In this report, we review and analyze the various principles, design considerations & fabrication processes for silicon piezoresistive based MEMS pressure sensor.

Tires can exhibit instabilities of low-level during inflation. Traditionally, it has been tricky and challenging to measure such instable small changes since they are generally dynamic pressures that are smaller in fraction of a *psi* which are superimposed on top of a high static pressure of 100 *psi* or greater. Some pressure sensors that are designed to measure large pressure of the order of 400 *psi* or greater may fail to capture lower resolution values since the signal generated from such low pressures are similar in magnitude to the ambient noise signals of the system and other error signals.

This research focuses on MEMS technology owing to its advantages such as miniature in size, low power consumption, less space requirement, low thermal expansion and easy to integrate and most important is, sensor developed is required to be placed between rim and tire bead for measurement of pressure in a critical area. In this research, a piezo resistive based MEMS pressure sensor have been designed, simulated, analyzed and fabrication process steps have been prepared and results are discussed.

Here following design parameters/ technical specifications have been considered:

1. Application: Bead seating pressure measurement in tire/ automobile

2. Size/ Type: Miniature/ MEMS based

3. Pressure range: 0-500 psi or 0-15 bar or 0-2.5MPa

4. Excitation: 5VDC±0.25VDC

5. Temperature: -40 to +125°C

6. Type of sensor: piezoresistive element in Wheatstone bridge configuration

7. Die size: 1600x1600Sqµm

8. Size of diaphragm: 500x500 Sqµm

9. Thickness of diaphragm: 25µm

10. Piezoresistive material: Polysilicon

11. Substrate material: n-type silicon substrate in <100> orientation

DESIGN PRINCIPLES & CONSIDERATIONS

A. Piezoresistive Effect

The basic principle of the device is: when a pressure is applied on the top of the membrane (diaphragm), the membrane deforms due to stress which leads to change in voltage at output, by change in the resistance of the piezoresistive element. By measuring the output voltage, the value of the pressure can be inferred. The resistance of the piezoresistive element will change by varying the pressure and the change in the output voltage are often read using the Wheatstone bridge circuit configuration. The phenomenon by which the electrical resistance of a material changes in response to mechanical stress is known as piezoresistivity [1]. Piezoresistivity in semiconductors is widely used in various sensors including accelerometers, cantilever force sensors, pressure sensors, and inertial sensors [2]. In stressed silicon, due to deformation there is a change in crystal potential distribution. Band diagram and the effective mass of the holes and electron is changed in turn due to this effect [3]. This leads to change in the carrier mobility which leads to a change in the resistance/ resistivity.

The resistivity change is calculated by using a 6 x 6 piezoresistive coefficient matrix and the stress tensor [1-4]. In silicon, due to the nature of its crystallographic structure, there are only 3 non-zero independent components (π_{11}, π_{12}, π_{44}) in the piezoresistive coefficient matrix as shown below:

$$\pi = \begin{bmatrix} \pi 11 & \pi 12 & \pi 12 & 0 & 0 & 0 \\ \pi 12 & \pi 11 & \pi 12 & 0 & 0 & 0 \\ \pi 12 & \pi 12 & \pi 11 & 0 & 0 & 0 \\ 0 & 0 & 0 & \pi 44 & 0 & 0 \\ 0 & 0 & 0 & 0 & \pi 44 & 0 \\ 0 & 0 & 0 & 0 & 0 & \pi 44 \end{bmatrix} \text{ -- (1)}$$

The simplified expression for resistance change in a piezoresistor is given by the following:

$$\frac{\Delta R}{R} = \pi l \sigma l + \pi t \sigma t \qquad \text{------------ (2)}$$

Where π_t and π_l are the transverse and longitudinal piezoresistive coefficients. σ_t and σ_l are the transverse and longitudinal stresses on the surface of the piezoresistors.

In piezoresistive pressure sensor, polysilicon has proven to be an excellent material for building up sensing elements. Presently, pressure sensors constitute the largest market segment of mechanical MEMS devices [5]. The most commonly used technique for measuring pressure involves applying pressure to one

side of a deformable diaphragm, a reference pressure to the other side, and determining how much the diaphragm deforms. There are several ways of sensing the deformation of a diaphragm across which a differential pressure has been applied. The pressure sensor example used in this paper uses an indirect, but very powerful way to sense the deformation by measuring the bending strain of the diaphragm. The sensing technique is based on a silicon property called piezoresistance, which is resistance that changes with stress (or strain). The resistivity of the material depends on the internal atom positions and motions. Strain changes these arrangements and, hence, the resistivity.

The effect of piezoresistivity in silicon can be largely enhanced by using ion implantation [6]. This technique is used to implant piezoresistive strain gauges in the diaphragm. In this research, piezo resistive type has been chosen instead of capacitive type because of its good linearity and high sensitivity.

B. The Proof Pressure and Burst Pressure

The proof pressure is typically accepted at 1.5 times the nominal/ required pressure of the sensor. The sensor is required to work up to this pressure while maintaining the overall required specifications [11]. Burst pressure is an important design parameter/ consideration for the diaphragm design, since this pressure limits the maximum stress/ load to which the diaphragm can be subjected [1]. This is the pressure at which the maximum stress σ_{max} on the diaphragm becomes equal to the critical stress σ_c which is actually the yield strength of the material. For the case of a single crystal silicon, σ_c=7GPa. Thus, for a square diaphragm having side length 2a and thickness, h, the burst pressure P_B is determined by substituting σ_{max}= σ_c in σ_{max}=and can be written as shown in (3).

$$P_B \left(\frac{a}{h}\right)^2 = \sigma_c$$ ------------------ (3)

Since the magnitude of maximum stress is larger in rectangular diaphragms, the burst pressure of the diaphragms having (L/W) > 1 is lower than the corresponding square diaphragm having (L/W) =1. This can, indeed, be seen from the Coventorware simulation results presented in Figure-2 for square diaphragms of different thicknesses t and varying length L, (i.e. L=500µm/ t=25 µm, L=750µm/t=37.5µm, L=1000 µm/t=50

µm, L=1200 µm/t=60 µm).

C. Dynamic Response of the Pressure Sensor

Over and above the static response and sensitivity, the frequency response of the pressure sensor is also an important consideration which becomes crucial in conditions where it is required to observe the changes in pressure over small intervals of time. Some examples are in bio applications such as the case of blood pressure (BP) or intracranial pressure (ICP) monitoring system [13]. The frequency response shows the ability of the sensing system to precisely respond to dynamic changes in pressure. The frequency response is governed by the sensing element that is the diaphragm which acts like a spring–mass system. The natural frequency of this pressure sensor is typically higher due to its small size and high Young's modulus of silicon value. With reference to the theory of plates, the resonance frequency of a clamped square diaphragm is given by the relation involving the diaphragm thickness h, width 2a, the material properties, which is represented as, Young's modulus E and the density ρ, as follows:

$$= 1.65 \frac{h}{a^2} \sqrt{\frac{E(1-v^2)}{\rho}}$$ --------------- (4)

Silicon Material properties assumption:

- Young's modulus: Ex = Ey =169 GPa, Ez =130 GPa
- Poisson's ratio: PRyz = 0.36, PRxy=0.064,PRxz=0.28
- Shear modulus: Gyz = Gxz = 79.6 GPa, Gxy=50.9 GPa

Considering the above design aspects, a MEMS pressure sensor was designed in Coventorware software with 2D schematic, 3D modeling, mapped grid meshing, simulation and analysis.

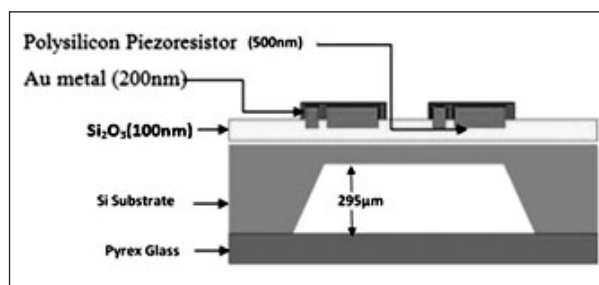The final structure of MEMS pressure sensor designed is as shown in Figure-1. The dimensions

Fig 1. Final Structure of MEMS Pressure Sensor

and materials have been arrived at after detailed analytical solution and simulation analysis studies.

2. MATHEMATICAL MODELING AND DESIGN CALCULATIONS

A. Diaphragm Dimension

The governing differential equation for deflection of thin plate (diaphragm) and small deflection is below:

$$\frac{\partial^4 w}{\partial x^4} + \frac{\partial^4 w}{\partial x^2 \partial y^2} + \frac{\partial^4 w}{\partial y^4} = \frac{P}{D} \quad \text{------------------ (5)}$$

where P is pressure, D is the bending rigidity [1]. By solving (5) with boundary conditions, where all sides of the sensor diaphragm are built-in, that is

$$w = 0, \frac{\partial w}{\partial n} = 0 \quad \text{------------------ (6)}$$

where 'n' is the normal vector direction along the sides of sensor diaphragm. The deflection of diaphragm can be expressed as:

$$w_1(x,y) = \frac{4PL^4}{\pi^5 D} \sum_{m=1,3,5} \frac{(-1)^{\frac{m-1}{2}}}{m^5} \cos(x') \times \left(1 - \frac{m' \tanh(m')+2}{2\cosh(m')} \cosh(y') + \frac{y'}{2\cosh(m')} \sinh(y')\right) \quad \text{....(7)}$$

$$w_2(x,y) = \frac{-2PL^4}{\pi^5 D} \sum_{m=1,3,5} c_m \frac{(-1)^{\frac{m-1}{2}}}{m^2 \cosh(m')} \times \left(f(x',y') + f(y',x')\right) \quad \text{---- (8)}$$

where L is diaphragm length, E is young's modulus, h is diaphragm thickness and v is Poisson's ratio, respectively. [22]

The maximum deflection of the diaphragm is at the center of diaphragm and is given as below:

$$w_{max} = w_1 + w_2$$

$$w_1(0,0) = 0.00406 PL^4/D, \; w_2(0,0) = -0.00280 PL^4/D$$

Therefore, $w_{max} = 0.00126 \, PL^4/D$

The consolidated graph of Deflection of the diaphragm Vs Pressure for varying thickness (different lengths) is shown in Figure-2. Here increase in deflection is noticed by increasing the thickness of diaphragm and applied pressure.

B. Burst Pressure

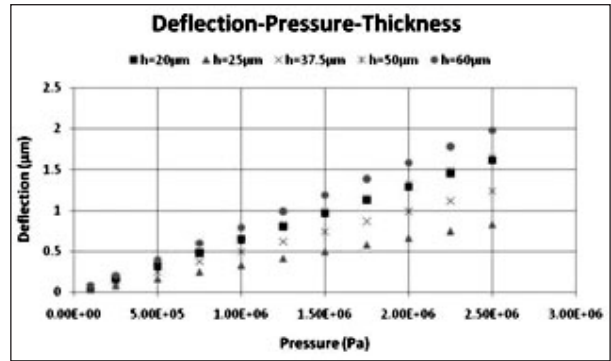The thicker and shorter diaphragm can have

Fig 2. Deflection-Pressure (with Varying Diaphragm Dimensions)

larger burst pressure. It can withstand more pressure on the wafer with decreasing in the diaphragm size. The thinner diaphragm means lower burst pressure and high sensitivity. In a single wafer many pressure sensors can be developed due to decrease in diaphragm size. Figure-3 indicates the burst pressure of the sensor for all 4 sensor models and that the deviation is insignificant. The maximum stress occurs at the middle of each edge of diaphragm. We can get maximum bending moment from

$$M_x = \frac{4 \, PL^2}{\pi^3} \sum_{m=1,3,5}^{\infty} \left(e_m (-1)^{\frac{m-1}{2}}\right) = -0.0513 PL^2 \quad \text{...(9)}$$

Substitute Eq9 in $\sigma_x = -6\frac{M_x}{h^2}$, we obtain

$$\sigma_{max} = 0.3078 \, P_{burst} \frac{L^2}{h^2}$$

The maximum nondestructive pressure is P_{burst}. It can be rewritten as $P_{burst} = 3.25\sigma_{max} h^2 / L^2$. On considering a diaphragm of thickness h=25 microns, the burst pressure is reduced from 15 MPa (15.00E+06 Pa) to 12 MPa (12.00E+06Pa) when the diaphragm length, L, is varied from 500µm to 1200µm as shown in Figure-3.
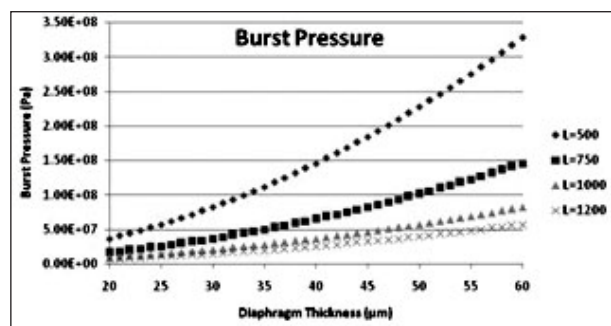

Fig 3. Burst Pressure Analysis Graph

C. Sensitivity

If the effect of piezoresistor length is neglected, the piezoresistor can be treated as a point at the middle of the diaphragm sides. Bending momentum is calculated by (9) and (10), respectively in x and y directions.

$$M_y = \frac{4vPL^2}{\pi^3} \sum_{m=1,3,5}^{\infty} e_m (-1)^{\frac{m-1}{2}} = -0.0513vPL^2 \quad (10)$$

For p-type piezoresistors oriented in the direction on a <100> diaphragm plane, which are connected in a Wheatstone bridge configuration, the parallel and perpendicular resistance changes due to the pressure-induced stress are expressed as

$$\left(\frac{\Delta R}{R}\right)_P = \frac{\pi_{44}}{2}(\sigma_t - \sigma_l) = -0.1539\pi_{44}(1-v)P\frac{L^2}{h^2} \quad (11)$$

$$\left(\frac{\Delta R}{R}\right)_v = \frac{\pi_{44}}{2}(\sigma_t - \sigma_l) = -0.1539\pi_{44}(1-v)P\frac{L^2}{h^2} \quad (12)$$

where σ_l and σ_t are longitudinal and transverse stress, respectively. The P is the piezoresistive coefficient defined along silicon crystallographic axes. Signal voltage output can be written in the form

$$\Delta V_o = V_C\left(\left(\frac{\Delta R}{2R}\right)_v - \left(\frac{\Delta R}{2R}\right)_P\right) = 0.1539\pi_{44}(1-v)P\left(\frac{L}{h}\right)^2 V_c \quad (13)$$

Sensitivity, S, can be expressed as

$$S = \frac{\Delta V_o}{V_c P} = 0.1539\pi_{44}(1-v)\left(\frac{L}{h}\right)^2 \quad .... (14)$$

The signal voltage output (ΔV_o) and sensor sensitivity (S) are proportional to the square of the ratio of the diaphragm length (L) to the diaphragm thickness (h). Figure-4 shows the sensitivity vs thickness analysis graph, i.e. the sensitivity of diaphragm for varying thickness (L & h). The higher ratio of L/h exhibits
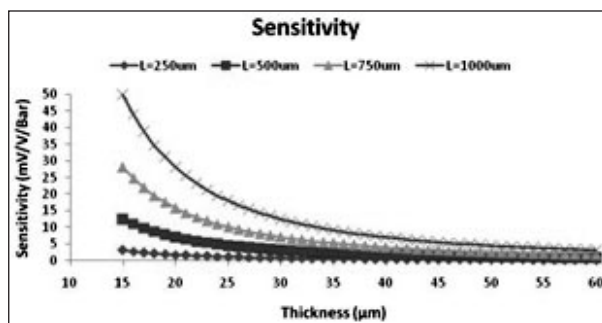

Fig 4. Sensitivity Analysis Graph

higher sensitivity, ie lower concentration has higher sensitivity. A thin and a long diaphragm have higher sensitivity.

Substituting burst pressure into (14), we can obtain

$$S\,P_{burst} = 0.5(1-v)\sigma_{max}\,\pi_{44} \quad ....(15)$$

D. Fabrication Process Flow

MEMS fabrication process steps for piezo resistive pressure sensor have been created as shown below: this is purely based on the fabrication facilities available at a particular foundry.

To start with a n-type 3 inch wafer of <100> orientation prime quality double side polished Si is taken and is cleaned by general and piranha cleaning process. In the first step possible Organic or Inorganic contaminations are removed from the wafer surface by a wet chemical cleaning treatment. Further the thickness of the wafer is reduced to 345 micron by KOH etching. Thermal oxidation process and LPCVD process are used to grow 600 nm oxide layers and 100nm of silicon nitride on both sides respectively. Photolithography is done on both sides to transfer pattern. Wet etching is done using TMAH on back side to form a cavity of 295 μm depth which is followed by etching Silicon Nitride & Silicon dioxide (Front & Back).

A Silicon dioxide layer of 100nm is deposited on the front side as an insulating layer followed by deposition of sensing element ie, Poly-Si layer of 500nm thickness using LPCVD process and lithography. Next step is at the front side, a conformal Silicon dioxide Si_2O_3 coating of thickness 500nm is done as a TSV liner for deep trench using PECVD. This is followed by UV Lithography and generic dry etching process using RIE for via opening (deep trench) for electrical contacts. Further metallization process is done by depositing Al/Au metal of thickness 200nm/2000Å as contacts pads using electro plating system. Later at the top, chemical mechanical polishing or planarization is done to remove unwanted conductive or dielectric materials on the silicon wafer, achieving a near-perfect flat and smooth surface upon which layers of integrated circuitry are built.

At the backside, the diaphragm cavity is sealed using Anodic bonding with Pyrex glass of thickness 75μm in vacuum in order to get an

absolute pressure sensor.

The final structure after fabrication is as shown in Figure-1

3. SIMULATIONS AND RESULTS

The simulation of design for the pressure sensor structure was carried out using CoventorWare® software for appropriate clamping conditions. The diaphragm deflection/displacement and the Misses stress distribution were measured for maximum pressure of for 2.5MPa (25bar) as shown in Fig 5to 9.

The edges of the pressure sensor were clamped with fixed faces/planes; however there is a fractional displacement at the edges on X & Y axis. We have focused on the Z displacement in Figure-6 and found that maximum displacement (up and down direction) is observed.

Figure-7 displays the node displacement in XYZ axis vs varying pressure till 2.5bar. It is observed that there is negligible movement on the XY axis since they are fixed. But the node displacement on the Z axis shows maximum displacement in up and down direction.

It is observed that the maximum diaphragm deflection is linearly proportional to applied pressure. In practice, the diaphragm thickness is about some 25 micrometers, and the deflection is much less than half of the diaphragm thickness. The length of the diaphragm is from some hundreds of micrometers to two thousand micrometers. The thin plate can be adopted in the design of pressure sensors [6] because the "ballon effect" will not occur [7]

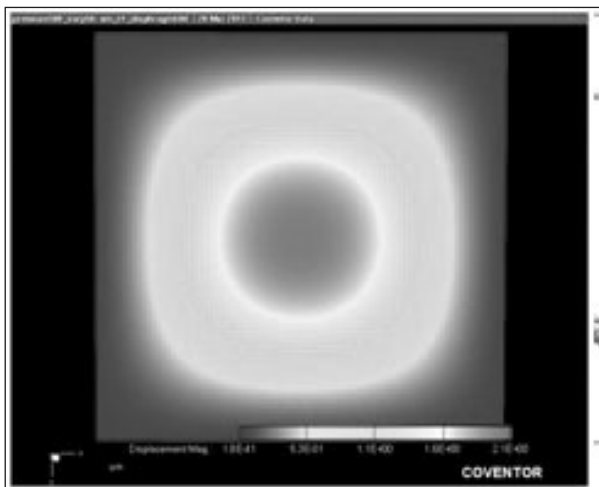Figure-8 shows the Von-Mises stress; it is

Fig 5. Displacement Magnitude in X & Y Axis
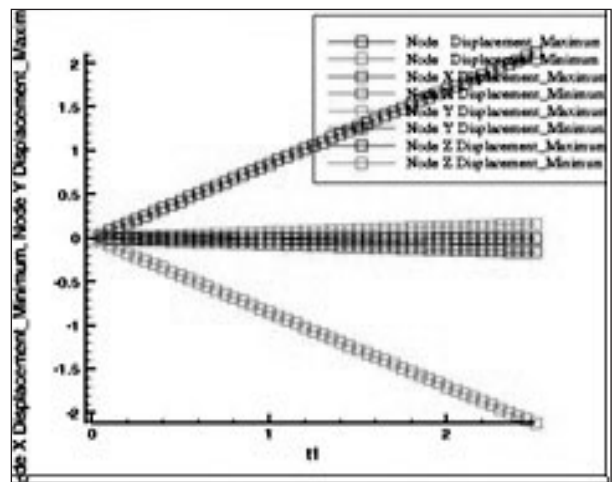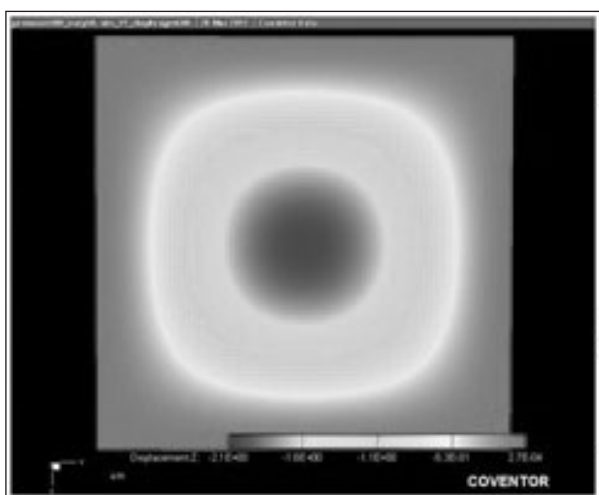

Fig 7. Displacement Graph

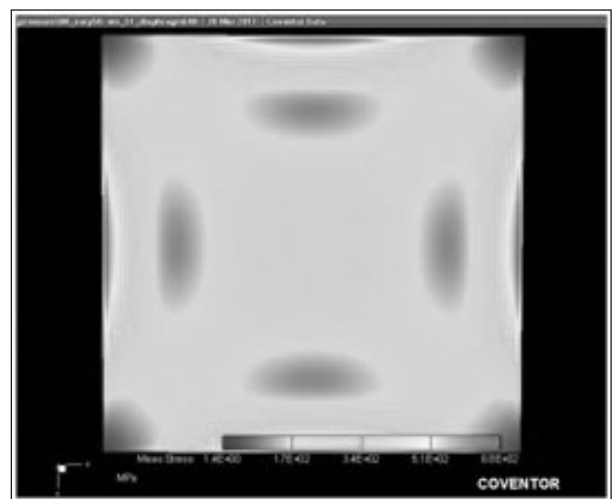Fig 6. Displacement Magnitude in Z axis

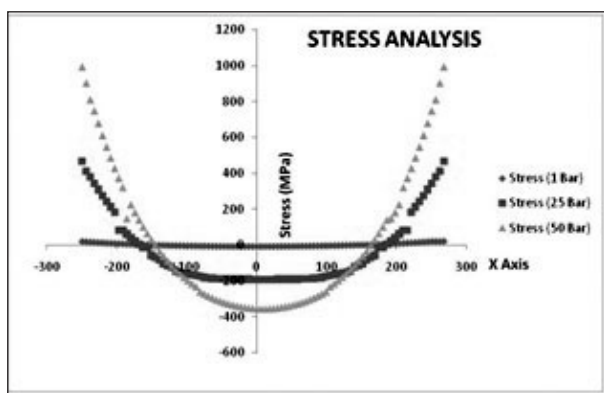Fig 8. Von-Mises Stress (L=400µm, t=25µm)
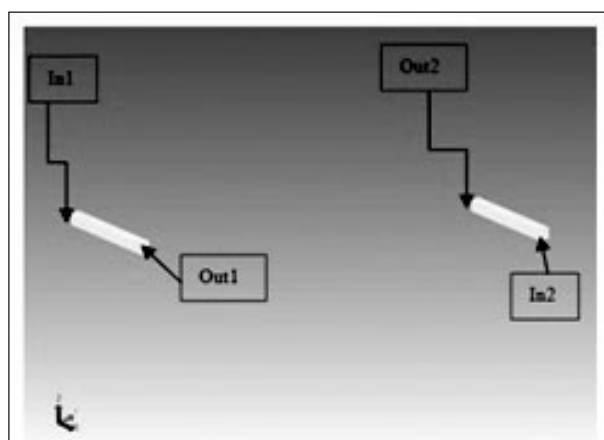
Fig 9. Stress Analysis Graph

Fig 10. Meshed Structure of PZR

observed that the stress is maximum at the centre of all four edges. Figure-9 represents the transverse stress component in the Y-axis direction, and X (width) is varied from -a to +a.

In a piezoresistive pressure sensor, the maximum tensile and compressive stress locations on the diaphragm surface are crucial to attain the maximum sensitivity by placing the resistors in precise locations. The piezoresistor placement is ideal to be of the length of the maximum stressed region and width with maximum stress penetration point on the diaphragm. Figure-9 shows the stress analysis where 3 different pressures of 1, 25 and 50 bar have been applied on the diaphragm of 25 microns thickness. It is observed that there is visible stress effect only when the length is beyond 400 microns. The stress at points near 200 microns on +ve and –ve axis are high compared to any other regions.

Using Coventorware software MemPZR solver, piezoresistive equations have been solved using a stress field from the Coventorware database, which is the result of MemMech

simulation carried out earlier. In this simulation MemPZR solver was used to investigate the output voltage as a function of pressure. As shown in Figure-10, two Piezoresistor 'pzr1' and 'pzr2' are used to simulate results, and their contact ends are named as in1, out1 and in2, out2 respectively for each pzr. These ends are subjected to the potential difference to simulate to voltage conditions in a connected circuit.

Table 1: Piezodomain Results

	patch voltage (V)	patch current (µA)	% change in current
in1	5	7.310123E08	4.430218E00
in2	5	6.66333E08	-4.809469E00
out1	0	-7.310134E08	4.430492E00
out2	0	-6.663329E08	-4.809597E00

The Table-1 displays the current sensed through the PZR parts when a 2.5bar of pressure and 5V of voltage is applied. The percentage change in current is with respect to the no-load condition. This change in current is due to the change in resistivity when the piezoresistor is subjected to stress.

4. CONCLUSION

In this paper an approach has been made to design, simulate, analyse and fabricate the MEMS based Piezoresistive Pressure Sensor for bead seating tire pressure measurement. Through this work, an overview on design methodology is discussed for silicon piezoresistive based square diaphragm pressure sensor. The design principles and fabrication process flow have been optimized based on the parameters discussed. They can be generalized for design of pressure sensors for different applications with different fabrication techniques and/or size and shape of different elements of the sensor. The designed sensor was simulated and analyzed in Coventorware software and also results validated through analytical solutions.

5. ACKNOWLEDGMENT

6. REFERENCES

1. K. N. Bhat and M. M. Nayak, MEMS Pressure Sensors- An Overview of Challenges in Technology and Packaging, Journal of Institute Of Smart Structures And Systems (ISSS), Vol. 2, No.1, pp39-71, March 2013

2. Bhat KN (2007) Silicon micromachined pressure sensors. J Indian Inst Sci 87(1):115–131, Bhat, K.N.,Vinoth Kumar, V.,Sivakumar, K., Madhavi, S.P., DasGupta, A., Rao, P.R.S., Bhattacharya, E., DasGupta, N. Manjula, S.R., Daniel, R.J., & Natarajan, K., 2006 "Silicon Micromachining for MOS Integrated Piezoresistive pressure Sensors with SOI approach," Indo-Japan Joint Seminar on 'Micro-Nano Manufacturing Science. Tokyo, pp. 19 - 26.

3. S. Santosh Kumar, B. D. Pant, Polysilicon thin film piezoresistive pressure microsensor: design, fabrication and characterization, Springer-Verlag Berlin Heidelberg 2014

4. S. Santosh Kumar and B. D. Pant, A Study of Analytical Solutions of Plate Equation for Pressure Microsensor Diaphragm: Limitations, Comparison and Usage, Journal of Microelectronics, Electronic Components and Materials Vol. 45, No. 1 (2015), 80–86

5. S. Santosh Kumar and B. D. Pant, Fabrication and Characterization of Pressure Sensor, and Enhancement of Output Characteristics by Modification of Operating Pressure Range, IEEE 2015

6. S. Santosh Kumar and B.D. Pant, Design of Piezoresistive MEMS Absolute Pressure Sensor, 16th International Workshop on Physics of Semiconductor Devices, Proc. of SPIE Vol. 8549 85491G-1

7. S. Santosh Kumar, Anuj K. Ojha, B. D. Pant, Experimental evaluation of sensitivity and non-linearity in polysilicon piezoresistive pressure sensors with different diaphragm sizes, Springer-Verlag Berlin Heidelberg 2014

8. S. Santosh Kumar, Anuj K. Ojha, Manish Kumar, and B. D. Pant, Comparative study of characteristics of polysilicon pressure sensor with different diaphragm sizes and piezoresistor configurations, Citation: 1724, 020094 (2016)

9. S. Santosh Kumar, B. D. (2014). Design principles and considerations for the 'ideal' silicon. Verlag Berlin Heidelberg: Microsyst Technol, Springer.

10. Tai-Ran Hsu. MEMS & Microsystems Design and Manufacture, China Machine Press: Beijing, 2002; pp. 284-289.

11. Thyagarajan V, Bhat KN (2013) Optimum location for piezoresistors with square diaphragm pressure sensor. In: Proceedings of 6th ISSS national conference on MEMS, smart material, structures and systems

12. Timoshenko, S. P., and S. Woinowski-Krieger, 1983, Theory of Plates and Shells, New York:McGraw- Hill.

13. Tsai HH, Hsieh CC, Fan CW, Chen YC, Wu WT (2009) Design and characterization of temperature-robust piezoresistive micropres- sure sensor with double-wheatstone-bridge structure. In: Pro- ceedings of the symposium on design, test, integration and pack- aging of MEMS/MOEMS, Rome, pp 363–368

14. Vandelli, N., 2008 "SiC MEMS Pressure Sensors For Harsh Environment Applications", MicroNano News , pp10-12 (April).

15. Vinoth Kumar, V., 2006 Design and Process Optimization for Monolithic Integration of Piezoresistive Pressure Sensor and MOSFET Amplifier with SOI Approach, MS Thesis, Electrical Engineering Department, Indian Institute of Technology, Madras, India.

16. Vinoth Kumar, V., A. DasGupta , K.N.Bhat and K. Natarajan, 2006, "Process Optimization for monolithic integration of piezoresistive pressure sensor and MOSFET Amplifier with SOI Approach," Journal of Physics Conference Series, Vol.34., pp. 210-215

17. Wong V.T.S. et al., 2000, "Bulk Carbon Nanotubes as Sensing Element for Temperature and Anemometry Micro Sensing", Proc. IEEE MEMS 2003, pp. 41- 44,

18. Fujitsuka N, Hamaguchi K, Funabashi H, Kawasaki e, Fukada T (2004) aluminum protected silicon anisotropic etching tech- nique using TMaH with an oxidizing agent and dissolved Si. R&D Rev Toyota CRDL 39(2):34–40

19. Fuller LF, Surdigo S (2003) Bulk micromachined pressure sensor. In: Proceedings of the 15th Biennial University/ Government/Indus- try Microelectronics Symposium, pp 317–320

20. Fung, C. K. M. ,Zhang M Q. H. Zhang , Dong Z., and Li, W. J., 2005, "Fabrication of CNT-Based MEMS Piezoresistive Pressure Sensors Using DEP Nano assembly" IEEE MEMS, pp.251-254.

21. Middlelhoek, S. & Audet, S.A., 1989, Silicon Sensors, San Diego, Academic Press.

22. Mohamed, N. M., Lai M. K. and Begam K. M., 2010, "Development of Aligned Carbon Nanotubes (CNTs) for Pressure Sensing Application", NSTI- Nanotech, Vol.2, 130-133

23. Mosser,V., Susuki,J.,Goss,J, & Obermeier, E., 1991, "Piezoresistive Pressure Sensors Based on Polycrystalline Silicon," Sensors and Actuators A,Vol.28, pp 113-132.

24. Narayanaswamy M, Daniel RJ, Sumangala K, Jeyasehar Ca (2011) Computer aided modelling and diaphragm design approach for high sensitivity silicon-on-insulator pressure sensors. Measure- ment 44:1924–1936 ◪

Kusuma N, Scientist-E, Sensor and Vision Technology Dept., Central Manufacturing Technology Institute, Bengaluru. She is having 26 years of professional experience in the field of Computerised Numerical Controllers (CNC)/Design & Development of Electrical Controllers for Special Purpose Machines (SPMs), Programmable Logic Controllers (PLC) programming, designing of MEMS Sensors, MEMS Fabrication process, MEMS Characterization process and Micro System Packaging processes. She has presented/published over 10 Papers in various National/ International Conferences/ journals.

Sujit Embrandiri S, M.Tech, Student, Electrical and Electronics Branch from Department of Instrumentation and Control Engineering, SRM University, Kattankulathur, TN. He did his MTech project work at CMTI during the year 2016 on the project "Peizo resistive MEMS Pressure Sensor for Tire Bead seating pressure measurement". (E-mail: sujit.embrandiri@gmail.com)